HHS Public Access

Author manuscript

Cerebellum. Author manuscript; available in PMC 2024 October 20.

Published in final edited form as:

Cerebellum. 2024 October ; 23(5): 1741–1753. doi:10.1007/s12311-023-01648-9.

Knockdown of the non-canonical wnt gene *Prickle2* leads to cerebellar Purkinje cell abnormalities while cerebellar-mediated behaviors remain intact

Parker W. Abbott[1,2], **Jason Hardie**[1,2], **Kyle P. Walsh**[1,2], **Aaron Nessler**[3], **Sean J. Farley**[4], **John H. Freeman**[1,2], **John Wemmie**[1,2], **Linder Wendt**[5], **Youngcho Kim**[2,6], **Levi Sowers**[2,7], **Krystal L. Parker**[1,2]

[1]Department of Psychiatry, The University of Iowa, Iowa City, Iowa, United States, 52242

[2]Iowa Neuroscience Institute, The University of Iowa, Iowa City, Iowa, United States, 52245

[3]Department of Biochemistry, The University of Iowa, Iowa City, Iowa, United States, 52245

[4]Department of Psychological and Brain Sciences, The University of Iowa, Iowa City, Iowa, United States, 52242

[5]Department of Biostatistics, The University of Iowa, Iowa City, Iowa, United States, 52245

[6]Department of Neurology, The University of Iowa, Iowa City, Iowa, United States, 52245

[7]Department of Pediatrics, The University of Iowa, Iowa City, Iowa, United States, 52245

Abstract

Autism spectrum disorders (ASD) involve brain wide abnormalities that contribute to a constellation of symptoms including behavioral inflexibility, cognitive dysfunction, learning impairments, altered social interactions, and perceptive time difficulties. Although a single genetic variation does not cause ASD, genetic variations such as one involving a non-canonical Wnt signaling gene, *Prickle2,* has been found in individuals with ASD. Previous work looking into phenotypes of *Prickle2* knock-out (*Prickle2*$^{-/-}$) and heterozygous mice (*Prickle2*$^{-/+}$) suggest patterns of behavior similar to individuals with ASD including altered social interaction and behavioral inflexibility. Growing evidence implicates the cerebellum in ASD. As *Prickle2* is expressed in the cerebellum, this animal model presents a unique opportunity to investigate the cerebellar contribution to autism-like phenotypes. Here, we explore cerebellar structural and physiological abnormalities in animals with *Prickle2* knockdown using immunohistochemistry, whole-cell patch clamp electrophysiology, and several cerebellar-associated motor and timing tasks, including interval timing and eyeblink conditioning. Histologically, *Prickle2*$^{-/-}$ mice have significantly more empty spaces or gaps between Purkinje cells in the posterior lobules and a decreased propensity for Purkinje Cells to fire action potentials. These structural cerebellar abnormalities did not impair cerebellar-associated behaviors as eyeblink conditioning and interval timing remained intact. Therefore, although *Prickle*$^{-/-}$ mice show classic phenotypes of ASD,

Corresponding Author: Krystal Parker, Ph.D, Associate Professor, Department of Psychiatry, Iowa Neuroscience Institute, University of Iowa, Iowa City, Iowa, 52242, krystal-parker@uiowa.edu.

they do not recapitulate the involvement of the adult cerebellum and may not represent the pathophysiological heterogeneity of the disorder.

Keywords

cerebellum; autism spectrum disorders; cognition; Purkinje cells; wnt signalling

Introduction

Autism Spectrum Disorders (ASD) involve neurodevelopmental impairments that are characterized by atypical social interactions, disrupted verbal and non-verbal communication, highly restricted interests, and repetitive behaviors [1]. Although these are core symptoms and identifying markers of ASD, they vary widely in their severity and presentation between affected individuals [2].

ASD is associated with a large degree of phenotypic heterogeneity, making it difficult to implicate specific brain regions or circuits in disease pathogenesis. Neuroanatomically, individuals with ASD have abnormalities in the anterior cingulate cortex, dorsolateral prefrontal cortex, medial frontal cortex, temporal lobe, parietal lobe, amygdala, and hippocampus among other regions [3–5]. These abnormalities include microstructural differences, altered connectivity between brain regions, and hyper- and hypoplasia of the developing brain [4]. Interestingly, the cerebellum is consistently abnormal in ASD and often includes a reduced density and size of Purkinje cells (PCs) throughout the cerebellum in postmortem analyses [6,7].

Along with studying ASD in the human brain, animal models have been pivotal to expanding our understanding of the cerebellum in ASD. Importantly, these models mimic human findings of Purkinje cell deficiencies and ASD-like behavior [8]. The Lurcher mouse model of Purkinje cell loss involves a gain of function mutation in the δ2 glutamate receptor gene. Lurcher mice display behaviors similar to humans with ASD including reduced behavioral flexibility, increased activity, and repetitive behaviors [9,10]. Additionally, a mouse deficient for tuberous sclerosis-I (TSC1) protein in Purkinje cells displays social deficits similar to individuals with ASD [11,12]. These results highlight the importance of the cerebellum and, specifically, the Purkinje cells in ASD.

Alongside the numerous brain regions contributing to ASD symptomology, many candidate genes have been identified, complicating our understanding of the etiology of the disorder [13,14]. A gene discovered in ASD, *Prickle2,* was first described in studies looking at interstitial microdeletions of chromosome 3p14. All but one of the individuals studied presented either a complete or partial deletion of *Prickle2* and all had marked intellectual disability and autism phenotypes [15,16]. Additionally, the *Prickle2* gene was characterized in a knockout mouse model and indicated as a potential model of ASD based on autism-like phenotypes [17]. Several characteristic autism-like behaviors were observed, including decreased behavioral flexibility, slower reversal learning, reduced social interest, and reduced dendritic arborization in the hippocampus contributing to impaired performance on hippocampus-dependent learning tasks such as contextual fear conditioning and Barnes

maze spatial memory learning. The role of the cerebellum in the pathophysiology of the ASD-like behavior in the *Prickle2* knock out mouse *(Prickle2* $^{-/-}$*)* was not considered.

PRICKLE2 is a planar cell polarity (PCP) protein in the non-canonical Wnt signalling pathway [17,18]. Murine PRICKLE2 protein is expressed in post-mitotic neurons and has been implicated in neuron maturation and neurite outgrowth via the Dishevelled dependent pathway [19–21]. *Prickle2* gene expression within the adult mouse brain is reported in the cerebral cortex, hippocampus, hypothalamus, midbrain, and cerebellum. Silencing or downregulating the *Prickle2* gene decreases neurite outgrowth in mouse neuroblastoma Neuro2a cell line preparations [22]. Cell-type specificity of *Prickle2* expression is not as well known.

Prickle2 is present within the mouse cerebellum at embryonic day 17.5, but its involvement in cerebellar development related to ASD pathology remains to be addressed [21]. Here, we investigated the effect of *Prickle2* knockdown on the structure and functional roles of the adult mouse cerebellum, including timing and motor-mediated tasks, that are implicated in ASD.

Methods

Prickle2 mutant mice

Gene targeting in TT2 embryonic stem cells was used to generate the *Prickle2* mutant mice (Acc. No. CDB0435K) [23] as described (http://www.cdb.riken.go.jp/arg/protocol.html). Mice are currently available as cryopreserved embryos through the Riken BioResearch Resource Center (mPk2, BRC number RBRC09345). The *Prickle2* mutant mouse line was backcrossed onto the C57bl6/J greater than 10 generations [17]. In total, 39 (28 male, 11 female) *Prickle2*$^{+/+}$ and *Prickle2*$^{-/-}$ littermates aged 4–5 months with a body weight of at least 17 g were included in this study. Animals were fed traditional rodent diet (Teklad) and housed in groups of 3–5 animals per cage without enrichment. Access to food and water were provided *ad libitum*, except for interval timing experiments where food was restricted to serve as performance motivation (see methods, Interval Timing Task). Cages were kept in rooms that had a 12-hr light cycle (0600 lights on, 1800 lights off). Sexes were combined due to no significant sex effects. These experiments were approved by the University of Iowa Institutional Animal Care and Use Committee and adhered to the NIH Guide for the Care and Use of Laboratory Animals. Genotyping was performed using PCR (For WT, Primer1: 5’-GAC CTC ATC TAC TTT TAC CAA-3’; Primer2: 5’-TAC TAC CAC CCA CTT TAT TCT-3’. For KO, Primer3: 5’-GGC TCT TTA CTA TTG CTT TAT-3’; Primer2: 5’-TAC TAC CAC CCA CTT TAT TCT-3’).

Immunohistochemistry

Mice (6 male *Prickle2*$^{+/+}$ and 5 male *Prickle2*$^{-/-}$*)* were intracardially perfused with PBS followed by 4% paraformaldehyde. The brain was removed and post-fixed in paraformaldehyde overnight. The brain was then stored in 30% sucrose for one day to allow for cryopreservation, indicated by the brain sinking to the bottom of the vial. Brains were sectioned in 40 μm increments on a cryostat (Leica) and stored in cryo-protectant

(50% PBS, 20% glycerol, 30% ethylene glycol) at −20 ºC. Slices were mounted and dried overnight before beginning immunostaining procedures. Primary antibodies Calbindin, a reliable marker of cerebellar Purkinje cells (anti-rabbit; Thermo Fisher; Millipore; 1:1000), GFAP (anti-rat; Thermo Fisher; 1:500) a marker of Bergmann glia, and DAPI (1:1000) for all neurons, were incubated on the tissue overnight at 4 ºC. Sections were visualized with Alexa Fluor fluorescent secondary antibodies (goat anti-rabbit IgG Alexa 488, goat anti-rat IgG Alexa 568, DAPI 504) and matched with the host primary by incubating for 2 hours. Images were captured using a Zeiss ApoTome.2 (Axio Imager M2). GFAP and DAPI was used for visualization of the Purkinje cells and cerebellar anatomy and were not quantified in these experiments.

Purkinje cell counting

Purkinje cell counts were obtained using Stereo Investigator software (MBF Bioscience, Williston, VT) using the optical fractionator [24]. We restricted our analysis to the vermis due to known vermal hypoplasia in ASD [25–27]. Sagittal cerebellar sections spanning 8 slices to the left and right of the midline (16 total at 40 μm; 640 μm total width of the midline cerebellum) were divided into the cerebellar lobules. Contours were drawn around the Purkinje cell layer of each lobule and randomized locations within a generated grid within the contours were selected by the optical fractionator algorithm. Only cells within the counting frame were included.

Purkinje cell gapping

In the same histological preparations for cell counting, lines were drawn within the Stereo Investigator software to measure the pixel length of each lobule and to measure the perimeter of the lobule. Gaps between calbindin-positive Purkinje cells were then measured and averaged for each lobule. Pixels were then converted to micrometers.

Patch clamp electrophysiology

300-μm parasagittal cerebellum vermis brain slices from adult male animals (7 animals; 4 *Prickle2*$^{+/+}$, 3 *Prickle2*$^{-/-}$) were prepared following previously established protocols [28]. Briefly, the cerebellum was dissected from 8- to 12-week-old mice in ice-cold slicing buffer (225 mM sucrose, 26 mM NaHCO3, 1.2 mM KH2PO4, 1.9 mM KCl, 10 mM d-glucose, 1.1 mM CaCl2, and 2 mM MgSO4) bubbled with 95% O2 and 5% CO2. Prepared slices were transferred to oxygenated artificial cerebrospinal fluid (aCSF) (127 mM NaCl, 26 mM NaHCO3, 1.2 mM KH2PO4, 1.9 mM KCl, 10 mM d-glucose, 2.2 mM CaCl2, and 2 mM MgSO4) at 32°C for 1 hour or more, then transferred to a submersion recording chamber perfused with aCSF at 32–34°C a rate of approximately 3 ml/min. Whole-cell recordings of Purkinje neurons were performed using 2.5- to 4-MΩ pipettes. Current-clamp recordings were obtained using a MultiClamp 700B Microelectrode Amplifier (Molecular Devices) and analyzed offline with GraphPad Prism. Scripts are available via GitHub (https://github.com/jhardie2017/jClamp). Experiments were discarded if access resistance varied by more than 20%. Tonic current was injected to hold the membrane voltage stable at −65 mV, and depolarizing current was injected in 50 pA increments. Data are from 1–3 cells per animal and are plotted as averaged recordings from each cell (≥3 recordings per cell). The numbers of cells and recordings per animal are located in Supplementary Table 1.

Motor function

A separate cohort of mice were tested for basic motor impairments, first using distance traveled in an open field, then observing ability to maintain speed with an accelerating rotorod, and finally using time to transverse a balance beam. All motor assays were conducted during the animals' light cycle.

Open field

Mice (7 male and 3 female *Prickle2*$^{+/+}$, 4 male and 8 female *Prickle2*$^{-/-}$) were placed in a 43.2 cm x 43.2 cm x 30.5 cm open field arena (Med Associates) for 10 minutes to assess distance traveled in the arena. Behavior was monitored using real time video imaging via a camera placed above the arena that was synced with CinePlex Studio (Plexon, Dallas, TX) allowing center of mass tracking. The open field test allows for the observation of the animals as they explore unfamiliar terrain and perform general locomotor activity. The distance traveled was calculated using MATLAB (Mathworks).

Rotarod

Mice (7 male and 3 female *Prickle2*$^{+/+}$, 4 male and 8 female *Prickle2*$^{-/-}$) were tested on an accelerating rotarod apparatus (Med Associates, St Albans, VT) consisting of a motor powered rotating rod that accelerated in speed of rotation over time to assess motor learning. For these trials the rotarod was set to accelerate from 4 to 40 rpm over the course of five minutes after which 40 rpm was maintained until the end of the trial. Motor testing was analyzed based on the length of time the animal could maintain running on the rod as it accelerated. Rodents were tested three times per day (at least 15 minutes between trials) for three days by placing them on the rod and recording latency to fall or failure to maintain running for two consecutive rotations should the mouse not independently fall off. The trials were stopped at 500 seconds if the animals did not fall.

Balance Beam

Mice (7 male and 3 female *Prickle2*$^{+/+}$, 4 male and 8 female *Prickle2*$^{-/-}$) were tested on a balance beam (84 cm x 1.2 cm x 1.2 cm) as an additional test of motor coordination and balance. The setup of the balance beam apparatus included a dark enclosure at one end of the beam and an open box at the other end that mice were placed into at the start of the trial. As mice prefer darkness over light and open spaces, they are motivated to transverse the beam to reach the dark enclosure on the opposite end. Time to traverse the beam was recorded over three days with three trials per day.

Delay eyeblink conditioning

Mice (12 male animals; 5 *Prickle2*$^{+/+}$, 7 *Prickle2*$^{-/-}$) were trained on delay-275 millisecond eyeblink conditioning. First, animals underwent surgery under isoflurane anesthesia for implantation of electromyographic (EMG) nickel wires and stimulating nickel wires, as described previously [29]. We chose to perform this more invasive eyeblink conditioning approach to capture dynamics of the task that are difficult to record using infrared cameras and air puff conditioning, and it has been successfully performed in mice [30,31]. The 2 EMG wires were threaded through the eyelid muscle (orbicularis oculi) and connected via

gold pins to a plastic connector. The Teflon coating was stripped near the eyelid to allow for electrical contact with the eyelid to measure eyeblink muscle activity. The 2 shock wires were implanted subdermally, immediately caudal to the left eye. The full assembly was then grounded to a stainless-steel skull screw and cemented with dental acrylic. Animals were then given a 1-week recovery period before starting the conditioning. Mice were connected to a lightweight cable that allowed for free movement inside of the conditioning chamber (BRS/LVE, Inc.). Testing was conducted during the light cycle.

Eyeblink conditioning was performed by repeatedly pairing a conditioned stimulus (CS-blue LED) with an aversive periorbital shock for the unconditioned stimulus (US; Figure 4A). Conditioned responses (CRs) were recorded as EMG signals from the nickel wires. A conditioning session was comprised of 100 trials, with a probe trial occurring after every 10 trials. One session lasted approximately 1 hour, depending on the length of each randomized intertrial interval. Each trial was separated by a randomized intertrial interval between 15 and 40 seconds. Responses that occurred 100 ms after the CS were considered startle responses and were excluded. Mice were trained for 8 sessions or more to reach criterion. Once mice reached criterion of 80% CRs in a single session, they started extinction training where only the CS was presented without the US shock to reduce the association between the CS and US over time. Data were collected using MATLAB scripts for extracting EMG traces, time-locking to events, and quantifying CR properties of latency, amplitude, and timing.

Interval timing task

Mice (7 male and 3 female *Prickle2*$^{+/+}$, 4 male and 8 female *Prickle2*$^{-/-}$) motivated by 85–90% food restriction were tested on a 12 second fixed interval timing task (Figure 5A). Training was performed in an operant chamber (MedAssociates) equipped with a nose poke port containing a yellow LED light (ENV-313W), a pellet dispenser (ENV-203–20), and a house light (ENV-315W). The entire configuration was housed in sound-attenuating chambers (MedAssociates). Nose pokes and the acquisition of rewards were recorded using infra-red beam breaks as the mouse accessed the reward nose poke port. First, animals learned that poking their nose into the nose poke port released their food pellets (20-mg rodent purified pellets, F0071, BioServe). Next, the mice were trained in a 12 second fixed-interval timing task. Rewards were delivered for nose pokes made after 12 seconds had elapsed from the time the nose poke port was illuminated to indicate the trial start. The mice were not punished for responding early but lack of responding for 18 seconds resulted in trial termination and the illuminated nose poke turned off with no reward administered. For rewarded nose pokes, the house light illuminated and remained lit until the animal collected the reward. Between each trial was a 24 ± 6 second pseudorandom interval after which the nose poke hole re-illuminated to indicate the start of a new trial. These trials were repeated for 60 minutes.

To assess interval timing performance we analyzed response efficiency, response start-times, number of responses and number of rewards. Response efficiency, indicating how well an animal estimated the interval, was analyzed as the number of well-timed responses between 11 and 12 seconds divided by the overall number of responses during the 12 second trial.

Efficiency scores closer to 1 reflect a greater number of responses occurring near the to-be-timed interval, indicating more temporally guided performance [32,33]. Single-trial start times were also analyzed as mice begin by responding at a constant, low rate on individual trials and increases responses in anticipation of reward. Time-response histograms were normalized to total responses to accurately demonstrate timing regardless of response rate.

Statistics

Statistical calculations were performed using GraphPad Prism 9 and SPSS. Data are visualized as mean ± SEM. Data were tested for normality using a Shapiro-Wilk test. When data were not normally distributed, a non-parametric statistical test was used. All histological comparisons were performed within-lobule due to size differences between each lobule, and an unpaired t-test was used for analysis. In the patch clamping data set, the frequency values were analyzed via a two- repeated measures ANOVA; baseline potential, fast afterhyperpolarization, resistance, and capacitance were analyzed with a two-tailed t-test. Behavioral testing was compared using a one-way ANOVA for data sets that occurred in one day and repeated-measures 2-way ANOVA for data sets that spanned multiple days. An alpha level of 0.05 was used for all assessments.

Results

Immunohistochemistry

Immunohistochemical analysis of vermal cerebellar sections for the expression of calbindin indicated no significant differences in the overall number of Purkinje cells between the *Prickle2*$^{-/-}$ and *Prickle2*$^{+/+}$ mice (6 male *Prickle2*$^{+/+}$ and 5 male *Prickle2*$^{-/-}$) (Figure 1A;1B). However, although posterior lobules (VI-X) had the same number of gapping or space between positively labeled Purkinje cells (Figure 1C), there was a significant difference in the length of the gaps (Figure 1D, multiple t-tests per lobule; IV,V $p = 0.006$; VI $p = 0.037$; VII $p = 0.0004$; VIII $p = 0.03$; IX $p = 0.02$; X $p = 0.012$). There were no differences for the total length of the perimeter within each lobule (Figure 1E).

Patch clamp electrophysiology

Given the prior characterization of Purkinje cell abnormalities in ASD and our finding of increased length of gaps between Purkinje cells in *Prickle2*$^{-/-}$ animals, we used whole-cell patch clamp electrophysiology to define their function (Figure 2A). Purkinje cells recorded from acute sagittal cerebellar vermal slices revealed typical high-frequency trains of action potentials in both *Prickle2*$^{-/-}$ *and Prickle2*$^{+/+}$ animals when injected with current, and output frequency was statistically significant (7 animals; 4 *Prickle2*$^{+/+}$, 3 *Prickle2*$^{-/-}$) (2-way ANOVA, current-by-genotype, $p = 0.0067$; main effect for current, $p < 0.0001$; main effect for genotype, $p = 0.0019$) (Figure 2B). A post hoc analysis indicates that the means for current input between 500–800 pA and 1100–1500 pA were significant (Sidak post hoc, Table 2). The baseline membrane potential was unchanged in the *Prickle2*$^{-/-}$ *mice* (Figure 2C). Interestingly, the peak of the fast afterhyperpolarization was significantly depolarized in *Prickle2*$^{-/-}$, thus the Purkinje cells have less hyperpolarization following an action potential (Figure 2D, unpaired two tailed t-test, $p = 0.0169$). The membrane resistance, baseline

potential, and capacitance of the Purkinje cells in the *Prickle2*$^{-/-}$ vermal cerebellar sections were not significantly different (Figure 2E-F). Thus, Purkinje cells of *Prickle2*$^{-/-}$ mice were less excitable and were unable to maintain firing frequencies that were comparable to *Prickle2*$^{+/+}$ animals when driven by current injection.

Motor Function

Performance of *Prickle2* mice was assessed on the open field test, the balance beam test, and the rotarod test revealing no statistically significant differences between genotypes (7 male and 3 female *Prickle2*$^{+/+}$, 4 male and 8 female *Prickle2*$^{-/-}$) (Figure 3A; 3B; 3C). Despite the observed Purkinje cell abnormalities, there were no gross motor impairments. There was a sex effect observed between male and female animals on the rotarod (repeated measures ANOVA, $p = 0.002$, main effect of sex). Sidak post hoc analysis indicates that this effect was largely driven by performance on Day 1 between female and male *Prickle2*$^{-/-}$ animals.

Eyeblink Conditioning

Prickle2$^{-/-}$ and *Prickle2*$^{+/+}$ animals were both able to acquire delay eyeblink conditioning (12 male animals, 5 months old; 5 *Prickle2*$^{+/+}$, 7 *Prickle2*$^{-/-}$) (2-way ANOVA, time-by-genotype, $p = 0.1240$; Figure 4A) and extinguish the learned responses with no differences between the genotype (2-way ANOVA, time-by-genotype, $p = 0.1342$; Figure 4B). Additionally, there were no significant differences in the CR amplitude, CR duration, CR latency, or percent of startle responses (Figure 4C-F).

Interval Timing

The efficiency of timing estimation on the 12-second fixed interval timing task (Figure 5A-B) was not statistically different between *Prickle2*$^{+/+}$ and *Prickle2*$^{-/-}$ mice (7 male and 3 female *Prickle2*$^{+/+}$, 4 male and 8 female *Prickle2*$^{-/-}$) (Figure 5C). The animals did not differ on the total number of responses (Figure 5D), the average time they started responding over the training days (Figure 5E), or the number or rewards obtained (Figure 5F).

Discussion

A full or partial deletion of PRICKLE2, a planar cell polarity (PCP) protein in the non-canonical Wnt signalling pathway, is associated with intellectual disability and autism phenotypes [15,16]. Although *Prickle2* is present within the mouse cerebellum at embryonic day 17.5, and continuous research heavily implicates the cerebellum in ASD pathology, our results suggest that brain wide knockdown of Prickle2 does not affect cerebellar-mediated tasks that are associated with ASD, despite our observations of abnormal gapping between Purkinje cells [7,21].

Purkinje cells are normally arranged in a layer between the granular and molecular layers of the cerebellum. Purkinje cells are the sole output of the computations that take place in the cerebellar cortex, relaying activity to the deep nuclei which project out of the cerebellum to downstream brain structures like the thalamus [34]. Although the overall count of Purkinje cells is not significantly decreased in the *Prickle2*$^{-/-}$ mice, our results reveal a notable

gapping between Purkinje cells in the posterior cerebellar vermis. The posterior cerebellar lobules of the vermis have been shown to be involved in emotional regulation [35,36].

Given that PRICKLE2 has been implicated in neuron maturation and neurite outgrowth via the Dishevelled dependent pathway, our results showing potential misplacement of Purkinje cells outside the appropriate Purkinje cell layer may be consistent [19–21]. The polarity of cells is established with the involvement of Dishevelled non-canonical Wnt signaling, where PRICKLE1 and PRICKLE2 proteins are thought to be involved in the proximal side of a cell during polarity processes. However, whether the specific role that PRICKLE2 plays in planar cell polarity could have driven the Purkinje cell gapping requires future studies [18]. There is recent evidence from vascular endothelial cells that describes a role for non-canonical Wnt signaling in cellular mechanocoupling [37]. Although Purkinje cells are not mechanically linked together, they do have a vital relationship with neighboring cells through ephaptic coupling that when disrupted, could alter migration patterns during development [38]. Although our data do not support a significant loss of Purkinje cells in the posterior cerebellar vermis, alterations in migration patterns could underly the gapping between Purkinje cells in the Purkinje cell layer. These findings are not consistent with reports of vermal Purkinje cell loss in individuals with ASD [7,26].

Purkinje cells of *Prickle*$^{-/}$ were less excitable than *Prickle2*$^{+/+}$ mice as evidenced by the I-F curve (Figure 2B). That is, they generated fewer action potentials for a given excitatory drive. With no stark behavioral changes related to the cerebellum, the differences we observed in the electrophysiology of Purkinje cells could be attenuated downstream to account for normal cerebellar-mediated behavior. Testing this would require looking at downstream areas that receive cerebellar input such as the thalamus to determine whether there is still proper functioning despite the decreased Purkinje cell firing frequency. It is well known that sustained Purkinje cell firing is certainly necessary for proper downstream signaling and learning [39,40]. One potential aspect of the Purkinje cell that could be impaired in *Prickle2*$^{-/-}$ mice comes from recent work that shows Purkinje cell afterhyperpolarizations are mediated by BK-type potassium channels, which when downregulated decreases action potential frequency [41,42]. This would fit with our current evidence, given that the fast afterhyperpolarization was more depolarized and produced lower firing frequencies. However, testing BK channels directly would be required to confirm whether they are driving the effect, and therefore remains speculative.

It is not known how non-canonical Wnt signaling could play a role in the dynamics of action potentials in Purkinje cells. There is some evidence to indicate a role that Wnt signaling plays in ion channel dynamics which could account for differences in action potentials. Several potassium and calcium channels have been shown to effect Wnt signaling. If Wnt signaling was disrupted, it is possible that ion channels that play a role in metabolic pathways could respond to that feedback and operate differently than normal physiological states [43]. Future Purkinje cell electrophysiological experiments that probe ion channel function through pharmacology or calcium imaging, are needed to define the role of calcium channel activity and potential dysfunction in *Prickle2*$^{-/-}$ mice. Subdividing the Purkinje cells in *Prickle2*$^{-/-}$ mice could provide further insight into the functional differences and implications of gapping in the Purkinje cell layer.

There are several limitations to this study. We combined sexes in the motor behavior and interval timing to sufficiently power our analysis. Although there were limited sex effects (Day 1, Rotorod), more samples would be required to make proper assessments of sex effects. Our focus on the cerebellar vermis may not accurately reflect the structural abnormalities reported in humans with ASD and many animal models given recent evidence localizing cognitive function to the lateral cerebellar hemispheres [11,44,45]. Post-mortem analysis of cerebellar tissue in individuals with ASD commonly reveals a loss of Purkinje cells, largely localized to the lateral hemispheres, as well as ectopic Purkinje cell localization outside of the Purkinje cell layer [5,44,46,47]. Additionally, Purkinje cells at the base of the primary fissure of hemispheric Lobule VI (HVI) are known to be critical for proper eyeblink conditioning [48–50]. Further, aldolase-C/Zebrin II striping of the cerebellum could provide further specificity to the lobular organization of Purkinje cell migration and affected function in the *Prickle2*$^{-/-}$ mice [51].

The cerebellum is necessary for learning and error detection [52]. Therefore, more robust differences may be identified by analyzing of nuanced aspects of a cerebellar-dependent learning. For eyeblink conditioning, longer interstimulus intervals could be used to make the task more challenging or trace conditioning could be included. Trace eyeblink conditioning differs from delay conditioning where there is co-termination of the CS and US by introducing a separation between the CS and US. This type of learning has been shown to involve long term memory and downstream brain circuits that receive input from the cerebellum like the thalamus and ultimately the cerebral cortex [53]. This may be essential as abnormal function of the cerebrocerebellar pathway is implicated in a myriad of neuropsychiatric illnesses like schizophrenia. During interval timing, previous work from our lab has reported inconsistent results from inactivation of the lateral cerebellar nucleus with muscimol [54,55]. Given the role for the cerebellum in learning, studies investigating cerebellar involvement in *Prickle2*$^{-/-}$ mice on the interval timing task may still be warranted at developmental timepoints, or with altered temporal durations, cues, or expected responses timing.

Overall, our results suggest that although *Prickle2* and associated PRICKLE2 protein expression in other brain regions is critical for ASD-relevant behaviors, it may not be critical for ASD-relevant behaviors that rely on the cerebellum in adult animals [17]. Given the heterogeneity of ASD in animal models of- and humans with- ASD, cerebellar abnormalities and impairment on cerebellar-mediated tasks may be expected to vary in severity and involvement.

Supplementary Material

Refer to Web version on PubMed Central for supplementary material.

References

1. Geschwind DH, & Levitt P. (2007). Autism spectrum disorders: Developmental disconnection syndromes. Current Opinion in Neurobiology, 17(1), 103–111. 10.1016/j.conb.2007.01.009 [PubMed: 17275283]

2. Bryson SE, & Smith IM (1998). Epidemiology of autism: Prevalence, associated characteristics, and implications for research and service delivery. Mental Retardation and Developmental Disabilities Research Reviews, 4(2), 97–103. 10.1002/(SICI)1098-2779(1998)4:2<97::AID-MRDD6>3.0.CO;2-U

3. Amaral DG, Schumann CM, & Nordahl CW (2008). Neuroanatomy of autism. Trends in Neurosciences, 31(3), 137–145. [PubMed: 18258309]

4. Donovan APA, & Basson MA (2017). The neuroanatomy of autism—A developmental perspective. Journal of Anatomy, 230(1), 4–15. 10.1111/joa.12542 [PubMed: 27620360]

5. Palmen SJMC (2004). Neuropathological findings in autism. Brain, 127(12), 2572–2583. 10.1093/brain/awh287 [PubMed: 15329353]

6. Bailey A, Luthert P, Dean A, Harding B, Janota I, Montgomery M, Rutter M, & Lantos P. (1998). A clinicopathological study of autism. Brain: A Journal of Neurology, 121 (Pt 5), 889–905. [PubMed: 9619192]

7. Fatemi SH, Aldinger KA, Ashwood P, Bauman ML, Blaha CD, Blatt GJ, Chauhan A, Chauhan V, Dager SR, Dickson PE, Estes AM, Goldowitz D, Heck DH, Kemper TL, King BH, Martin LA, Millen KJ, Mittleman G, Mosconi MW, … Welsh JP (2012). Consensus paper: Pathological role of the cerebellum in autism. Cerebellum (London, England), 11(3), 777–807. 10.1007/s12311-012-0355-9 [PubMed: 22370873]

8. Mapelli L, Soda T, D'Angelo E, & Prestori F. (2022). The Cerebellar Involvement in Autism Spectrum Disorders: From the Social Brain to Mouse Models. International Journal of Molecular Sciences, 23(7), 3894. 10.3390/ijms23073894 [PubMed: 35409253]

9. Dickson PE, Rogers TD, Mar ND, Martin LA, Heck D, Blaha CD, Goldowitz D, & Mittleman G. (2010). Behavioral flexibility in a mouse model of developmental cerebellar Purkinje cell loss. Neurobiology of Learning and Memory, 94(2), 220–228. 10.1016/j.nlm.2010.05.010 [PubMed: 20566377]

10. Martin LA, Goldowitz D, & Mittleman G. (2010). Repetitive behavior and increased activity in mice with Purkinje cell loss: A model for understanding the role of cerebellar pathology in autism. European Journal of Neuroscience, 31(3), 544–555. 10.1111/j.1460-9568.2009.07073.x [PubMed: 20105240]

11. Stoodley CJ, D'Mello AM, Ellegood J, Jakkamsetti V, Liu P, Nebel MB, Gibson JM, Kelly E, Meng F, Cano CA, Pascual JM, Mostofsky SH, Lerch JP, & Tsai PT (2017). Altered cerebellar connectivity in autism and cerebellar-mediated rescue of autism-related behaviors in mice. Nature Neuroscience, 20(12), 1744–1751. 10.1038/s41593-017-0004-1 [PubMed: 29184200]

12. Tsai PT, Hull C, Chu Y, Greene-Colozzi E, Sadowski AR, Leech JM, Steinberg J, Crawley JN, Regehr WG, & Sahin M. (2012). Autistic-like behaviour and cerebellar dysfunction in Purkinje cell Tsc1 mutant mice. Nature, 488(7413), 647–651. 10.1038/nature11310 [PubMed: 22763451]

13. Geschwind DH (2011). Genetics of autism spectrum disorders. Trends in Cognitive Sciences, 15(9), 409–416. 10.1016/j.tics.2011.07.003 [PubMed: 21855394]

14. Muhle R, Trentacoste SV, & Rapin I. (2004). The genetics of autism. Pediatrics, 113(5), e472–486. [PubMed: 15121991]

15. Maria Christina Schwaibold E, Zoll B, Burfeind P, Hobbiebrunken E, Wilken B, Funke R, & Shoukier M. (2013). A 3p interstitial deletion in two monozygotic twin brothers and an 18-year-old man: Further characterization and review. American Journal of Medical Genetics Part A, n/a-n/a. 10.1002/ajmg.a.36129

16. Okumura A, Yamamoto T, Miyajima M, Shimojima K, Kondo S, Abe S, Ikeno M, & Shimizu T. (2014). 3p Interstitial Deletion Including PRICKLE2 in Identical Twins With Autistic Features. Pediatric Neurology, 51(5), 730–733. 10.1016/j.pediatrneurol.2014.07.025 [PubMed: 25193415]

17. Sowers LP, Loo L, Wu Y, Campbell E, Ulrich JD, Wu S, Paemka L, Wassink T, Meyer K, Bing X, El-Shanti H, Usachev YM, Ueno N, Manak RJ, Shepherd AJ, Ferguson PJ, Darbro BW, Richerson GB, Mohapatra DP, … Bassuk AG (2013). Disruption of the non-canonical Wnt gene PRICKLE2 leads to autism-like behaviors with evidence for hippocampal synaptic dysfunction. Molecular Psychiatry, 18(10), 1077–1089. 10.1038/mp.2013.71 [PubMed: 23711981]

18. Veeman MT, Axelrod JD, & Moon RT (2003). A Second Canon. Developmental Cell, 5(3), 367–377. 10.1016/S1534-5807(03)00266-1 [PubMed: 12967557]

19. Fujimura L, Watanabe-Takano H, Sato Y, Tokuhisa T, & Hatano M. (2009). Prickle promotes neurite outgrowth via the Dishevelled dependent pathway in C1300 cells. Neuroscience Letters, 467(1), 6–10. 10.1016/j.neulet.2009.09.050 [PubMed: 19788910]
20. Mrkusich EM, Flanagan DJ, & Whitington PM (2011). The core planar cell polarity gene prickle interacts with flamingo to promote sensory axon advance in the Drosophila embryo. Developmental Biology, 358(1), 224–230. 10.1016/j.ydbio.2011.07.032 [PubMed: 21827745]
21. Tissir F, & Goffinet AM (2006). Expression of planar cell polarity genes during development of the mouse CNS. The European Journal of Neuroscience, 23(3), 597–607. 10.1111/j.1460-9568.2006.04596.x [PubMed: 16487141]
22. Okuda H, Miyata S, Mori Y, & Tohyama M. (2007). Mouse Prickle1 and Prickle2 are expressed in postmitotic neurons and promote neurite outgrowth. FEBS Letters, 581(24), 4754–4760. 10.1016/j.febslet.2007.08.075 [PubMed: 17868671]
23. Yagi T, Tokunaga T, Furuta Y, Nada S, Yoshida M, Tsukada T, Saga Y, Takeda N, Ikawa Y, & Aizawa S. (1993). A Novel ES Cell Line, TT2, with High Germline-Differentiating Potency. Analytical Biochemistry, 214(1), 70–76. 10.1006/abio.1993.1458 [PubMed: 8250257]
24. Olesen MV, Needham EK, & Pakkenberg B. (2017). The Optical Fractionator Technique to Estimate Cell Numbers in a Rat Model of Electroconvulsive Therapy. Journal of Visualized Experiments, 125, 55737. 10.3791/55737
25. Carper RA (2000). Inverse correlation between frontal lobe and cerebellum sizes in children with autism. Brain, 123(4), 836–844. 10.1093/brain/123.4.836 [PubMed: 10734014]
26. Courchesne E, Yeung-Courchesne R, Press GA, Hesselink JR, & Jernigan TL (1988). Hypoplasia of cerebellar vermal lobules VI and VII in autism. The New England Journal of Medicine, 318(21), 1349–1354. 10.1056/NEJM198805263182102 [PubMed: 3367935]
27. Kaufmann WE, Cooper KL, Mostofsky SH, Capone GT, Kates WR, Newschaffer CJ, Bukelis I, Stump MH, Jann AE, & Lanham DC (2003). Specificity of Cerebellar Vermian Abnormalities in Autism: A Quantitative Magnetic Resonance Imaging Study. Journal of Child Neurology, 18(7), 463–470. 10.1177/08830738030180070501 [PubMed: 12940651]
28. Piochon C, Titley HK, Simmons DH, Grasselli G, Elgersma Y, & Hansel C. (2016). Calcium threshold shift enables frequency-independent control of plasticity by an instructive signal. Proceedings of the National Academy of Sciences, 113(46), 13221–13226. 10.1073/pnas.1613897113
29. Freeman JH, & Nicholson DA (1999). Neuronal activity in the cerebellar interpositus and lateral pontine nuclei during inhibitory classical conditioning of the eyeblink response. Brain Research, 833(2), 225–233. 10.1016/S0006-8993(99)01547-4 [PubMed: 10375698]
30. Lim R, Zaheer A, Khosravi H, Freeman JH Jr, Halverson HE, Wemmie JA, & Yang B. (2004). Impaired motor performance and learning in glia maturation factor-knockout mice. Brain Research, 1024(1–2), 225–232. 10.1016/j.brainres.2004.08.003 [PubMed: 15451385]
31. Wemmie JA, Chen J, Askwith CC, Hruska-Hageman AM, Price MP, Nolan BC, Yoder PG, Lamani E, Hoshi T, Freeman JH, & Welsh MJ (2002). The acid-activated ion channel ASIC contributes to synaptic plasticity, learning, and memory. Neuron, 34(3), 463–477. 10.1016/s0896-6273(02)00661-x [PubMed: 11988176]
32. Parker KL, Chen K-H, Kingyon JR, Cavanagh JF, & Narayanan NS (2015). Medial frontal ~4 Hz activity in humans and rodents is attenuated in PD patients and in rodents with cortical dopamine depletion. Journal of Neurophysiology, jn.00412.2015. 10.1152/jn.00412.2015
33. Parker KL, Ruggiero RN, & Narayanan NS (2015). Infusion of D1 Dopamine Receptor Agonist into Medial Frontal Cortex Disrupts Neural Correlates of Interval Timing. Frontiers in Behavioral Neuroscience, 9, 294. 10.3389/fnbeh.2015.00294 [PubMed: 26617499]
34. Voogd J. (1998). The anatomy of the cerebellum. Trends in Neurosciences, 21(9), 370–375. 10.1016/S0166-2236(98)01318-6 [PubMed: 9735944]
35. Pierce JE, Thomasson M, Voruz P, Selosse G, & Péron J. (2022). Explicit and Implicit Emotion Processing in the Cerebellum: A Meta-analysis and Systematic Review. The Cerebellum. 10.1007/s12311-022-01459-4
36. Schmahmann JD (2019). The cerebellum and cognition. Neuroscience Letters, 688, 62–75. 10.1016/j.neulet.2018.07.005 [PubMed: 29997061]

37. Carvalho JR, Fortunato IC, Fonseca CG, Pezzarossa A, Barbacena P, Dominguez-Cejudo MA, Vasconcelos FF, Santos NC, Carvalho FA, & Franco CA (2019). Non-canonical Wnt signaling regulates junctional mechanocoupling during angiogenic collective cell migration. eLife, 8, e45853. 10.7554/eLife.45853
38. Han K-S, Guo C, Chen CH, Witter L, Osorno T, & Regehr WG (2018). Ephaptic Coupling Promotes Synchronous Firing of Cerebellar Purkinje Cells. Neuron, 100(3), 564–578.e3. 10.1016/j.neuron.2018.09.018 [PubMed: 30293822]
39. Freeman JH (2015). Cerebellar learning mechanisms. Brain Research, 1621, 260–269. 10.1016/j.brainres.2014.09.062 [PubMed: 25289586]
40. Ito M. (2002). Historical Review of the Significance of the Cerebellum and the Role of Purkinje Cells in Motor Learning. Annals of the New York Academy of Sciences, 978(1 THE CEREBELLU), 273–288. 10.1111/j.1749-6632.2002.tb07574.x [PubMed: 12582060]
41. Dell'Orco JM, Pulst SM, & Shakkottai VG (2017). Potassium channel dysfunction underlies Purkinje neuron spiking abnormalities in spinocerebellar ataxia type 2. Human Molecular Genetics, 26(20), 3935–3945. 10.1093/hmg/ddx281 [PubMed: 29016852]
42. Niday Z, & Bean BP (2021). BK Channel Regulation of Afterpotentials and Burst Firing in Cerebellar Purkinje Neurons. The Journal of Neuroscience, 41(13), 2854–2869. 10.1523/JNEUROSCI.0192-20.2021 [PubMed: 33593855]
43. Muccioli S, Brillo V, Chieregato L, Leanza L, Checchetto V, & Costa R. (2021). From Channels to Canonical Wnt Signaling: A Pathological Perspective. International Journal of Molecular Sciences, 22(9), 4613. 10.3390/ijms22094613 [PubMed: 33924772]
44. Hampson DR, & Blatt GJ (2015). Autism spectrum disorders and neuropathology of the cerebellum. Frontiers in Neuroscience, 9. 10.3389/fnins.2015.00420
45. Shipman ML, & Green JT (2019). Cerebellum and cognition: Does the rodent cerebellum participate in cognitive functions? Neurobiology of Learning and Memory. 10.1016/j.nlm.2019.02.006
46. Bauman M, & Kemper TL (1985). Histoanatomic observations of the brain in early infantile autism. Neurology, 35(6), 866–866. 10.1212/WNL.35.6.866 [PubMed: 4000488]
47. Whitney ER, Kemper TL, Bauman ML, Rosene DL, & Blatt GJ (2008). Cerebellar Purkinje cells are reduced in a subpopulation of autistic brains: A stereological experiment using calbindin-D28k. Cerebellum (London, England), 7(3), 406–416. 10.1007/s12311-008-0043-y [PubMed: 18587625]
48. Attwell PJE, Rahman S, & Yeo CH (2001). Acquisition of Eyeblink Conditioning Is Critically Dependent on Normal Function in Cerebellar Cortical Lobule HVI. The Journal of Neuroscience, 21(15), 5715–5722. 10.1523/JNEUROSCI.21-15-05715.2001 [PubMed: 11466443]
49. Heiney SA, Kim J, Augustine GJ, & Medina JF (2014). Precise Control of Movement Kinematics by Optogenetic Inhibition of Purkinje Cell Activity. Journal of Neuroscience, 34(6), 2321–2330. 10.1523/JNEUROSCI.4547-13.2014 [PubMed: 24501371]
50. Steinmetz AB, & Freeman JH (2014). Localization of the cerebellar cortical zone mediating acquisition of eyeblink conditioning in rats. Neurobiology of Learning and Memory, 114, 148–154. 10.1016/j.nlm.2014.06.003 [PubMed: 24931828]
51. Brochu G, Maler L, & Hawkes R. (1990). Zebrin II: A polypeptide antigen expressed selectively by purkinje cells reveals compartments in rat and fish cerebellum. The Journal of Comparative Neurology, 291(4), 538–552. 10.1002/cne.902910405 [PubMed: 2329190]
52. Popa LS, & Ebner TJ (2019). Cerebellum, Predictions and Errors. Frontiers in Cellular Neuroscience, 12, 524. 10.3389/fncel.2018.00524 [PubMed: 30697149]
53. Weible AP, McEchron MD, & Disterhoft JF (2000). Cortical involvement in acquisition and extinction of trace eyeblink conditioning. Behavioral Neuroscience, 114(6), 1058–1067. [PubMed: 11142638]
54. Heslin KA, Purnell JR, De Corte BJ, & Parker KL (2022). A limited cerebellar contribution to suprasecond timing across differing task demands. Behavioral Neuroscience, 136(5), 479–494. 10.1037/bne0000531 [PubMed: 36222639]

55. Parker KL, Kim YC, Kelley RM, Nessler AJ, Chen K-H, Muller-Ewald VA, Andreasen NC, & Narayanan NS (2017). Delta-frequency stimulation of cerebellar projections can compensate for schizophrenia-related medial frontal dysfunction. Molecular Psychiatry. 10.1038/mp.2017.50

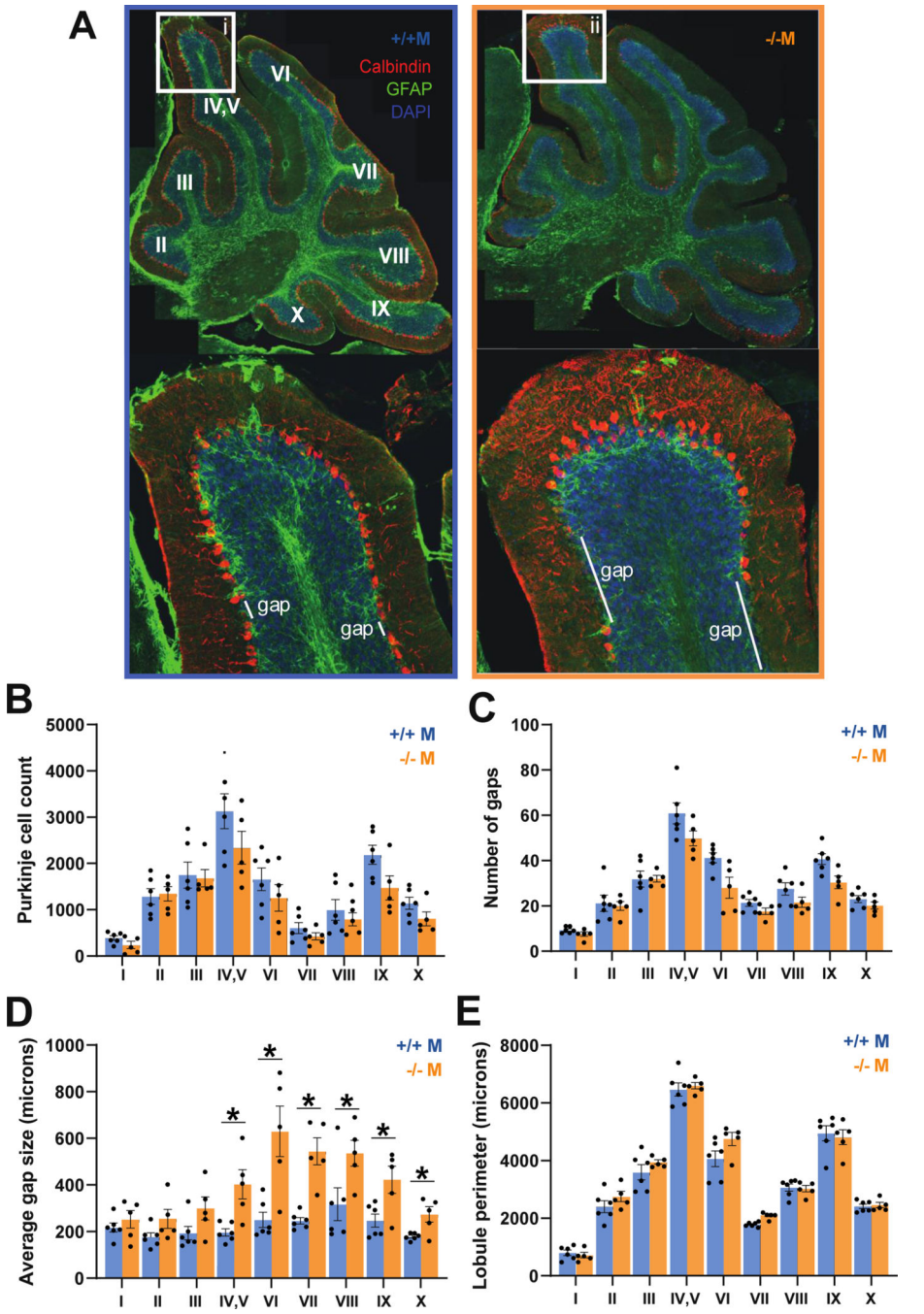

Figure 1.

Immunohistochemistry (6 male *Prickle2*$^{+/+}$, 5 male *Prickle2*$^{-/-}$). **A** Representative images of vermal immunohistochemical staining (top) with anti-Calbindin labeling of Purkinje cells (red), GFAP (green), and DAPI (blue) in *Prickle2*$^{+/+}$ and *Prickle2*$^{-/-}$mice with a zoomed in view of lobules IV,V (below). **B** The number of Purkinje cells and **C** the number of spaces between neighboring positively labeled Purkinje cells or gaps, in vermis lobules IV,V, VIII, IX, and X were not statically different (means ± SEM). Gaps can be seen in 1A. **D** The average size of the gaps, were significantly increased for the *Prickle2*$^{-/-}$ mice in lobules

IV/V, VI, VII, VIII, IX, and X (*$p < 0.05$) while **E** the overall length of the perimeter of the lobules was not statistically significant.

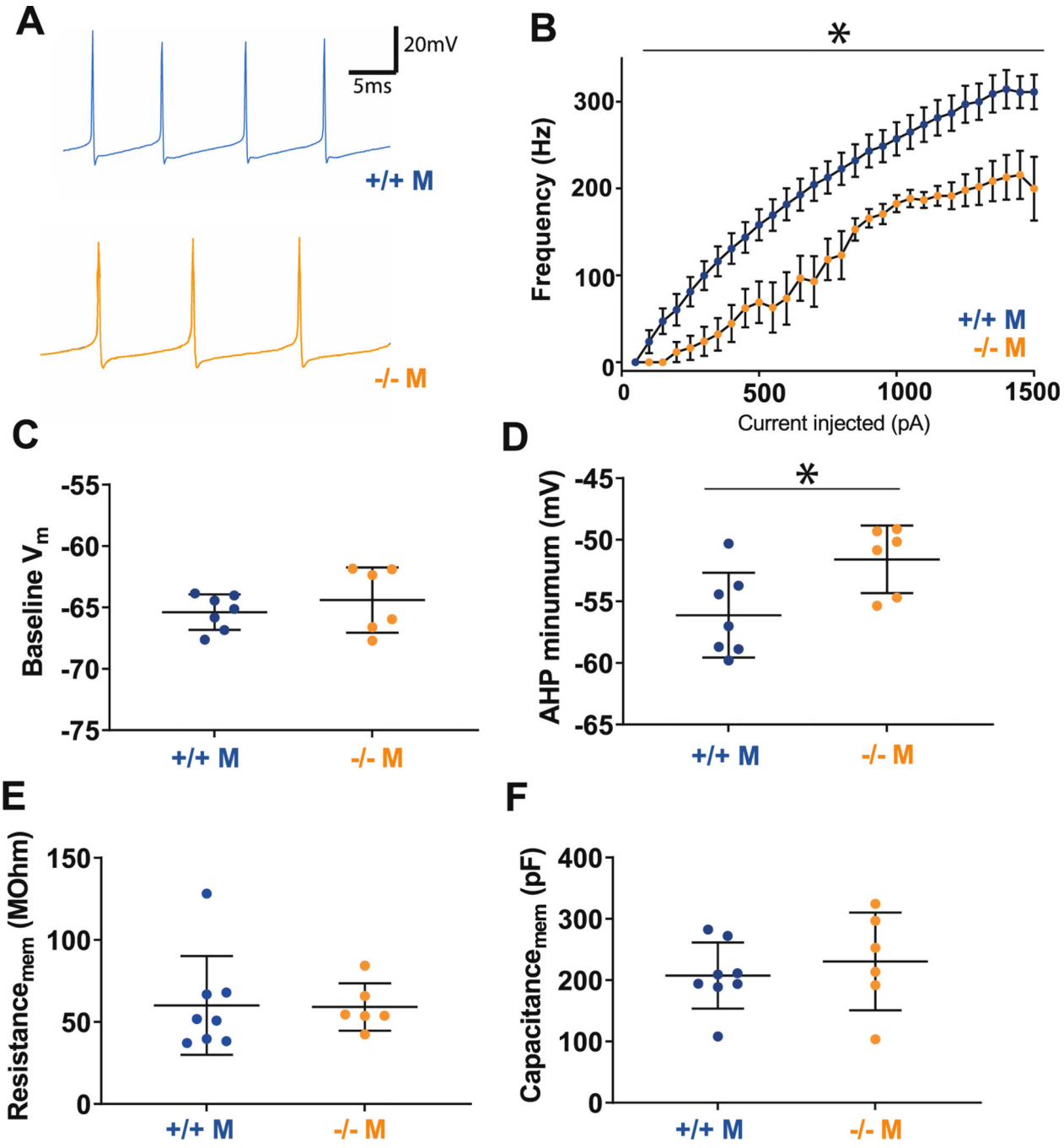

Figure 2.

Patch-clamp electrophysiology of vermal Purkinje cells. Data are from 1–3 cells per animal (n = 4 male WT, 3 male KO) and are plotted as averaged recordings from each cell (≥3 recordings per cell) **A** Representative traces of Purkinje cell action potentials recorded for *Prickle2*$^{+/+}$ (top) and *Prickle2*$^{-/-}$ *(bottom).* **B** Output frequency of action potentials in Purkinje cells was significantly different when increasing steps of current were injected to elicit action potentials. **C** Baseline resting membrane potentials were unchanged in *Prickle2*$^{-/-}$ Purkinje cells. **D** Fast afterhyperpolarization of the action potentials was

significantly less hyperpolarized in *Prickle2*$^{-/-}$ Purkinje cells while, **E** their membrane resistance and **F** capacitance was unchanged.

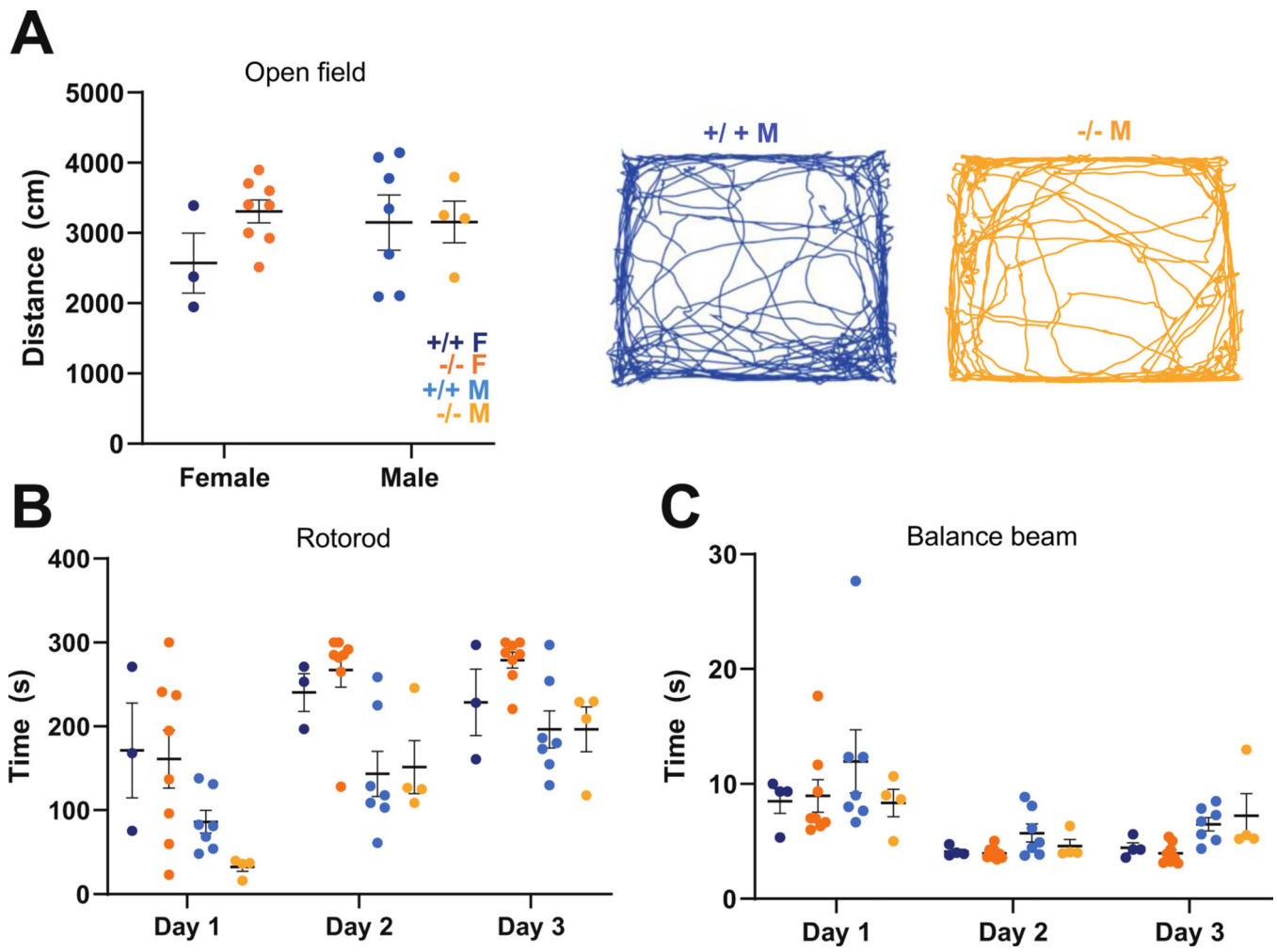

Figure 3.

Motor function (7 male and 3 female *Prickle2*$^{+/+}$, 4 male and 8 female *Prickle2*$^{-/-}$)**A** Total distance traveled during the 10 minutes of open field was not significantly different between the *Prickle2*$^{+/+}$ and *Prickle2*$^{-/-}$ animals (left), example open field movement traces (right). **B** While all animals learned to stay on the rotarod longer over each day of training and **C** time to cross the balance beam decreased, learning did not differ significantly between genotypes.

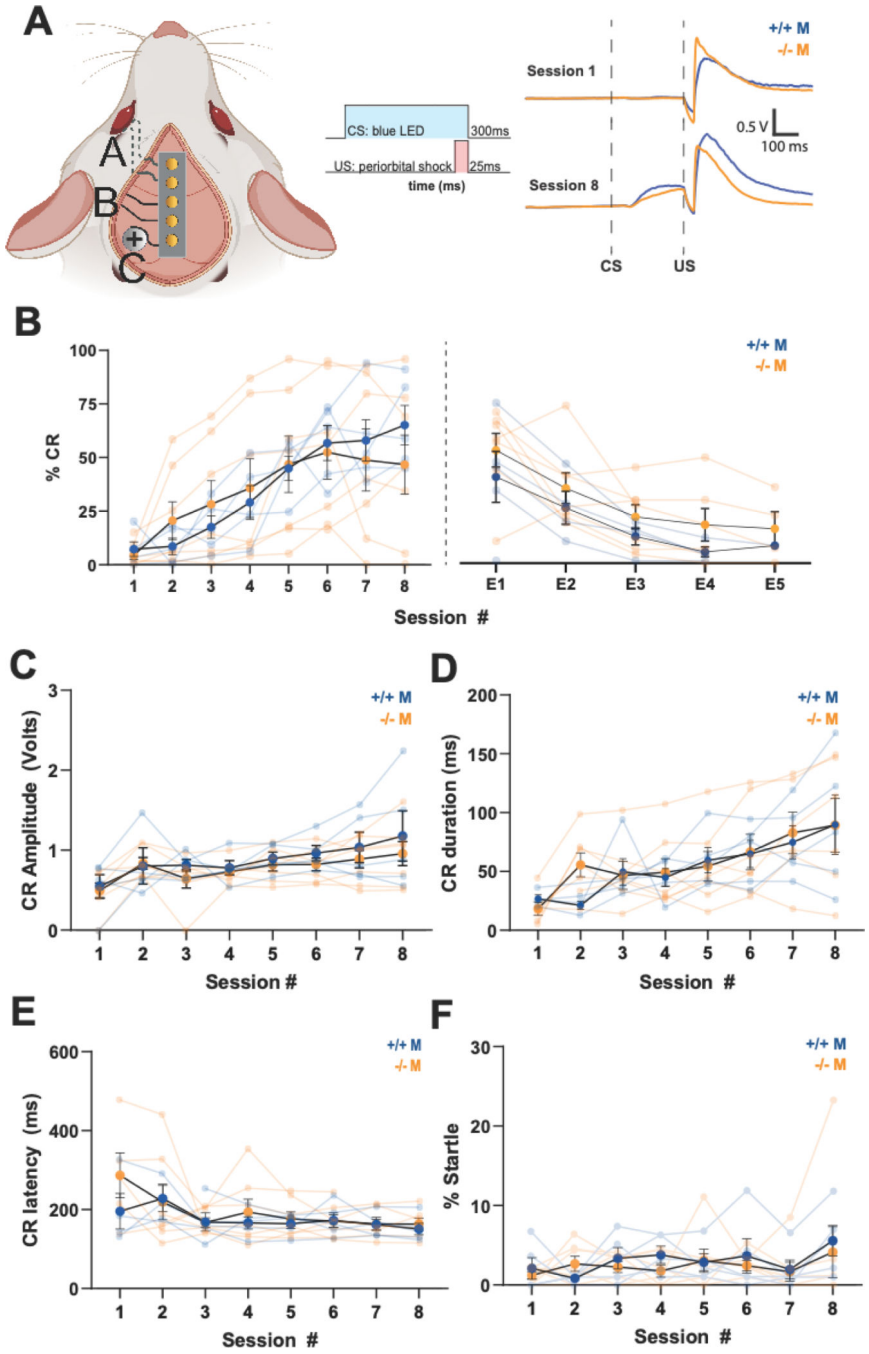

Figure 4.

Eyeblink conditioning (5 male *Prickle2*$^{+/+}$, 7 male *Prickle2*$^{-/-}$) **A** (left) Surgery schematic, A corresponds to the two EMG wires that are threaded through the eyelid; B corresponds to the shock wires; C corresponds to the ground screw (middle) Visualization of the stimuli used in the paradigm. A 300 ms blue LED coterminated with a 25 ms periorbital shock. (right) Averaged eyelid EMG trace from all animals of both genotypes for the first session and the eighth session **B** Percent CR for the 100 trials of the first nine sessions of paired CS and US trials (left) followed by extinction sessions with presentation of US alone.

There were no significant differences between the *Prickle2*$^{+/+}$ and *Prickle2*$^{-/-}$ on eyeblink conditioning as they both **C l**earned to express CRs in anticipation of the US **D** CR amplitude was not significantly different between *Prickle2*$^{+/+}$ and *Prickle2*$^{-/-}$ **E** the CRs had a similar latency to occur between the groups, and **F** they had a similar incidence of startle responses at the start of the trials (%).

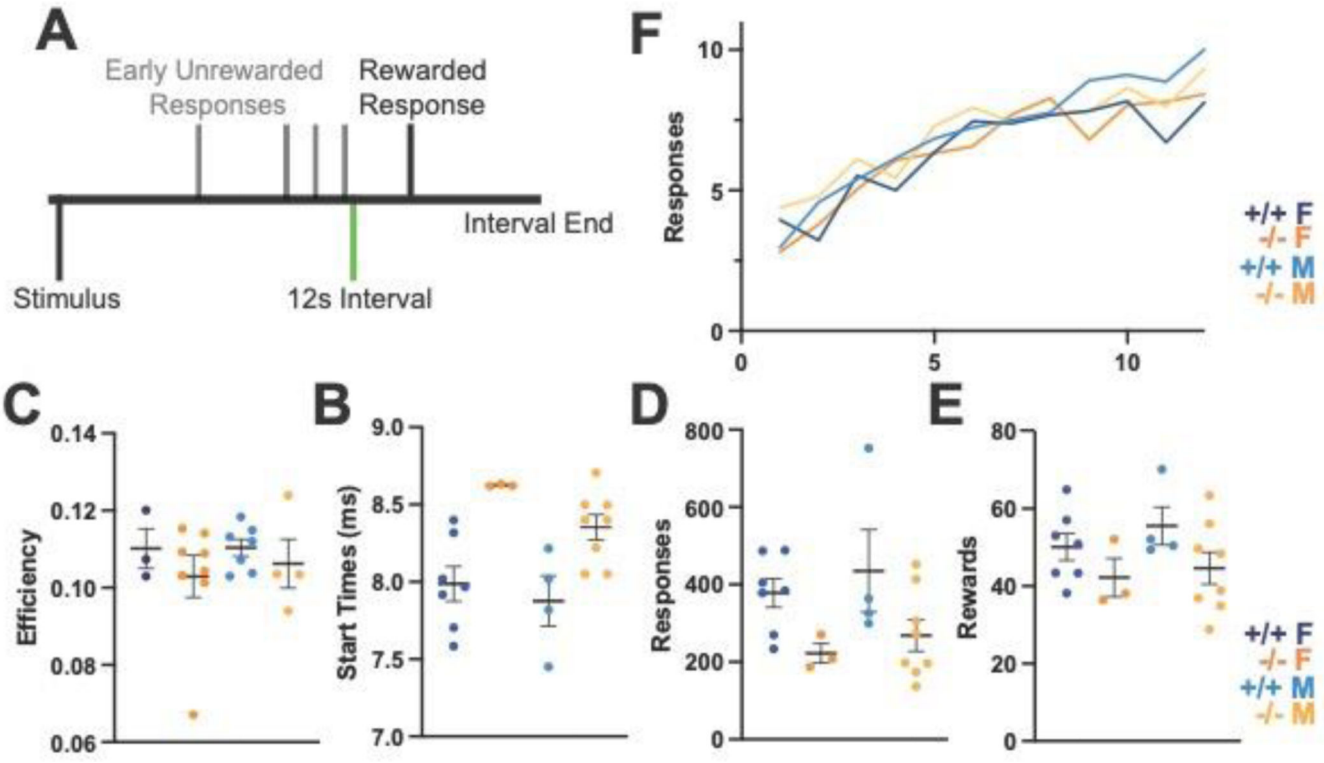

Figure 5.

Interval timing (7 male and 3 female *Prickle2*$^{+/+}$, 4 male and 7 female *Prickle2*$^{-/-}$).**A** Schematic of a single 12 s interval timing trial where there is an LED light that comes on in the response port indicating the start of the trial. Early pokes before the 12 s interval has elapsed are not rewarded or punished while rewards are provided for the first poke that occurs following the 12 interval. There were no significant differences between the *Prickle2*$^{+/+}$ and *Prickle2*$^{-/-}$ animals on the **B** number of responses over the interval or their **C** efficiency, **D** start times, **E** or rewards.

Table 1:

Histological Significant Statistical Analyses

Experiment	+/+ mean	Std. dev.	−/− mean	Std. dev.	Test	p-value
Gap size, lobule IV, V (Figure 1D)	196.215	39.343	402.61228	139.8067031	t-test	0.006847
Gap size, lobule VI (Figure 1D)	250.09	79.9126	793.22734	545.014055	t-test	0.037603
Gap size, lobule VII (Figure 1D)	246.0292	34.63034	544.252	129.1624976	t-test	0.000391
Gap size, lobule VIII (Figure 1D)	317.4604	172.8212	598.7834	189.4927221	t-test	0.02994
Gap size, lobule IX (Figure 1D)	247.3316	69.5714	529.59316	245.9357476	t-test	0.02397
Gap size, lobule X (Figure 1D)	178.4168	14.56501	273.72872	73.7383788	t-test	0.012189
Patch clamping, I-F (Figure 2B)					Two-way ANOVA	current-by-genotype, $p = 0.0067$; main effect for current, $p < 0.0001$; main effect for genotype, $p = 0.0019$)
Patch clamping, fast afterhyperpolarization (Figure 2D)	−56.12	3.438	−51.58	2.745	t-test	0.025